its actual geometric arrangement *the σ interaction between the olefin and the metal d orbitals is significantly more important than the π interaction with the d orbitals.*

Three types of molecular orbital calculations have been carried out to assess the relative σ and π bonding in Zeise's salt. An extended Hückel calculation concluded that σ and π bonding were of about equal importance.[4] The same conclusion was reached on the basis of a CNDO type calculation.[5] An Xα-SW calculation concluded that the π bonding is much less than the π bonding.[6] Because the transition energies calculated in these studies were all so far from those experimentally observed, the above conclusions are not of quantitative use.

6. Photochemical Consequences. The solution-phase photochemistry of Zeise's salt has been studied by Adamson et al.[27] The onset of photoreactivity began at about 26 000 cm^{-1} and reached the highest quantum yields for ligand substitution at 32 800 cm^{-1}. The authors attributed the ethylene aquation photoreaction to the lowest-energy singlet state.

The detailed assignment of the spectrum of Zeise's salt provides a straightforward, a posteriori interpretation of the photochemistry. The lowest ligand field transition populates the $d_{x^2-y^2}$ orbital. This orbital is most strongly σ antibonding between the platinum and the ethylene ligand, as shown by the l_σ parameters in Table IV. The photochemical loss of ethylene is thus most simply interpreted in terms of the large σ bond weakening between the platinum and ethylene in the excited state. The π-bonding changes in the excited state reinforce the bonding explanation of the photochemistry. The d_{xy} orbital which is depopulated in the lowest ligand field transition is π antibonding between the platinum and the chloride ligands. Thus the one-electron transition depopulates a π-antibonding orbital which strengthens the metal chloride π bonds. The major orbital factor governing the photochemistry is the population of the $d_{x^2-y^2}$ orbital, which is σ antibonding between the platinum and the ethylene.

(27) Natarajan, P.; Adamson, A. W., *J. Am. Chem. Soc.* **1971**, *93*, 5599.

Summary

Ligand field and charge-transfer electronic absorption transitions have been assigned in the low-temperature single-crystal polarized absorption spectrum. The lowest energy ligand field excited state arises from the d_{xy} to $d_{x^2-y^2}$ one-electron transition. This excited state undergoes a 0.23-Å distortion in the totally symmetric cis Pt–Cl stretching normal mode. Angular overlap parameters were determined. Ethylene is a strong σ donor (stronger than ammonia) and a weak π acceptor toward Pt(II).

Acknowledgment. The support of the National Science Foundation is gratefully acknowledged.

Registry No. Zeise's salt, 16405-35-9.

Localization and Transfer of Protons between ^{15}N Atoms of *meso*-Tetraphenylporphine Probed by Nuclear Overhauser Effects and Dipole–Dipole Relaxation Times

Jürgen Hennig and Hans-Heinrich Limbach*

Contribution from the Institut für Physikalische Chemie der Universität Freiburg i.Br., D-7800 Freiburg, West Germany. *Received December 27, 1982*

Abstract: The longitudinal relaxation times T_1 of the central and of the β-pyrrole protons of $^{15}N_4$-*meso*-tetraphenylporphine (TPP) dissolved in toluene-d_8 have been measured at 90.02 MHz, and the ^{15}N-T_1, including the Nuclear Overhauser Effects (NOE), at 9.12 MHz, both as a function of the temperature. A ^1H-T_1 minimum was observed at approximately 220 K. The data for the central protons could be explained by a superposition of two dipolar relaxation mechanisms, one involving the ^{15}NH and the other the central HH dipolar pair. The β-pyrrole proton data were consistent with a mutual dipolar relaxation mechanism of these protons. Below room temperature the thermally activated hydrogen tunneling process of the inner protons between the four nitrogen atoms is slow and the ^{15}N NMR spectra show two ^{15}N signals which arise from the protonated and the nonprotonated nitrogen atoms in accordance with the literature. Because of the proton exchange, these two signals have the same T_1 and the same negative NOE above 200 K. At lower temperatures, slow proton exchange causes an NOE breakdown of the nonprotonated nitrogen signal which is accompanied by different T_1 values for the two signals. The NOE of the NH signal breaks down at a lower temperature because of slow molecular tumbling. The Arrhenius curve of the hydrogen migration previously determined could be verified also at lower temperatures by a quantitative calculation of the NOE as a function of temperature. The protonated nitrogen is relaxed by dipole–dipole coupling to the inner proton. The intrinsic relaxation of the nonprotonated nitrogen could be described to a major extent by the chemical shift anisotropy relaxation mechanism and to a minor extent by direct dipole–dipole relaxation to the distant inner protons which yields a small negative NOE. Vibrationally averaged mean cubic distances of 1.02 Å for the inner NH bond and of 2.4 Å for the distance between the central protons, as well as a distance of about 2.5 Å between two closest β-pyrrole protons, were derived from the relaxation data without assumptions concerning the anisotropy of the molecular tumbling. The possibility of detecting small amounts of tautomers by NOE measurements is discussed.

Introduction

The problem of proton localization and transfer in hydrogen bonded systems is a matter of continuing theoretical and experimental interest.[1-24] In particular, the hydrogen migration in *meso*-tetraphenylporphine (TPP)[1-12] has attracted special attention.

(1) Limbach, H. H. "The Use of NMR Spectroscopy in the Study of Hydrogen Bonding in Solution", in "Aggregation Processes", Gormally, J.; Wyn-Jones, E., Ed., Elsevier: Amsterdam, 1983; Chapter 16.

(2) Storm, C. B.; Teklu, Y. *J. Am. Chem. Soc.* **1974**, *94*, 53. Storm, C. B.; Teklu, Y. *Ann. N.Y. Acad. Sci.* **1973**, *206*, 631.

(3) Abraham, R. J.; Hawkes, G. E.; Smith, K. M. *Tetrahedron Lett.* **1974**, 1483.

(4) Eaton, S. S.; Eaton, G. R. *J. Am. Chem. Soc.* **1977**, *99*, 1601.

(5) Gust, D.; Roberts, J. D. *J. Am. Chem. Soc.* **1977**, *99*, 3637.

0002-7863/84/1506-0292$01.50/0

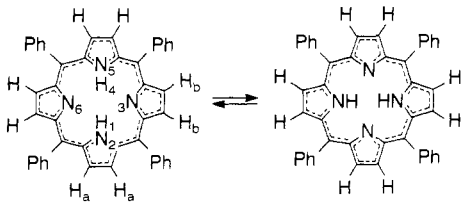

(1)

This reaction, discovered by Storm and Teklu,[2] was first interpreted in terms of transition state theory.[2-5] In a number of papers from our laboratory we have proposed that the migration takes place by tunneling between quantized NH-stretching states.[6-10] Evidence for this mechansim was obtained from a discussion of the activation parameters,[6,7] the kinetic HH/HD/DD isotope effects[8] which were measured by dynamic NMR spectroscopy for the first time for TPP as well as for the system acetic acid/methanol/tetrahydrofuran,[8,14,15] and from a discussion of the sharp NH stretching bands in TPP.[10] At low temperatures a considerable difference between the longitudinal relaxation times T_1 of the β-pyrrole protons and the corresponding relaxation times $T_{1\rho}$ in the rotating frame was found.[6,9] A possible explanation for this difference, originally attributed to the migration process,[6] is the fact that at low temperatures the minimum of T_1 is reached.[11] This prospect made TPP at low temperatures an excellent model for us for the simulation of slow tumbling biomolecules containing NH···N hydrogen bonds where it is often difficult to localize the protons.[17-20] The measurement of T_1 relaxation times or of (^{1}H^{15}N) Nuclear Overhauser Effects (NOE) can lead to a determination of the proton loci.[21-24] However, the influence of the kinetics of proton excahnge on the NOE has not yet been taken into account in a quantitative way. Therefore, we undertook the present combined study of ^{1}H-T_1, ^{15}N-T_1 relaxation times and of (^{1}H^{15}N) NOE of ^{15}N$_4$-TPP dissolved in toluene-d_8 in order to learn something about the influence of the known hydrogen migration exchange rates on the relaxation behavior of TPP and in order to explore whether such measurements can be used to determine the hydrogen positions.

The ^{15}N relaxation data will be interpreted in terms of a dominant ^{1}H^{15}N dipole–dipole relaxation and magnetization transfer between the ^{15}N atoms caused by the HH migration. A quantitative analysis provides very slow hydrogen exchange rates as well as the NH and the HH distance which are difficult to determine by X-ray analysis in the solid state.[25-29]

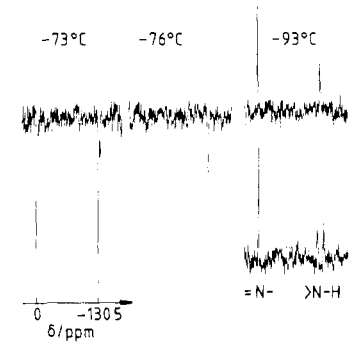

Figure 1. ^{15}N NMR spectra of a saturated solution of ^{15}N$_4$-TPP in toluene-d_8 at different temperatures and 9.12 MHz. Upper traces: ^{1}H decoupled spectra, lower trace: undecoupled spectrum; 5000 scans, 90 pulse length, 5 s repetition time, sweep width 2000 Hz, 5 Hz line broadening. At −73 °C the low-field signal (nonprotonated atoms) and the upfield signal (protonated atoms) experience the same Nuclear Overhauser Effect by magnetization transfer arising from the proton exchange. At lower temperatures the NOE of the low-field signal breaks down due to slow proton exchange. The NOE breakdown of the upfield signal arises because of slow molecular tumbling.

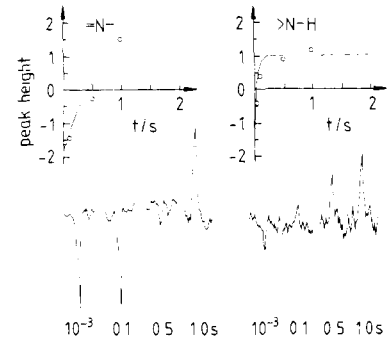

Figure 2. Inversion recovery ^{15}N-T_1 experiment on the two ^{15}N signals of ^{15}N$_4$-TPP in toluene-d_8 at 180 K and 9.12 MHz. Left: low-field; right: upfield signal; conditions as in Figure 1. The curves were calculated by using eq 24 and 25.

Experimental Section

^{15}N$_4$-TPP was synthesized according to Adler et al.[30] using ^{15}N pyrrole (95%, CEA, Orsay, France) as starting material. Toluene-d_8 (Merck, Darmstadt) was dried over sodium–potassium alloy. The sealed NMR samples with a diameter of 10 mm were prepared on a vacuum line as described previously.[6] The NMR experiments were performed with a Bruker CXP 100 FT NMR pulse spectrometer operating at 90.02 MHz for ^{1}H and at 9.12 MHz for ^{15}N. The sample temperatures were measured with a low-temperature thermometer caibrated against the chemical shifts of a pure methanol sample.[31] As described previously,[6,8,12,13] the room temperature signal of the central protons of ^{15}N labeled TPP consists of a pentet at high field because the hydrogen migration is fast. A value of $\delta = -2.3$ ppm was found for toluene-d_8 as solvent which is about 1 ppm at lower field compared to tetrahydrofuran-d_8.[6] At low temperatures the hydrogen migration is slow and the signal consists of a doublet.[6,8,12,13] We have previously described the line shape as a function of the proton exchange rates.[6] The signal of the β-pyrrole protons (H_a and H_b in eq 1) consists of a singlet at room temperature and of two singlets ($\delta = 8.91$ ppm and 9.05 ppm) at low temperatures.[2-6] T_1 measurements were performed on the signals of the central and the β-pyrrole protons using the inversion recovery technique.[32]

In order to obtain a better signal to noise ratio of the ^{15}N NMR spectra, the length of the RF coil in the multinuclear 10-mm probe which

(6) Hennig, J.; Limbach, H. H. *J. Chem. Soc., Faraday Trans. 2* **1979**, *75*, 752.
(7) Limbach, H. H.; Hennig, J. *J. Chem. Phys.* **1979**, *71*, 3120.
(8) Limbach, H. H.; Hennig, J.; Gerritzen, D.; Rumpel, H. *Faraday Discuss. Chem. Soc.* **1982**, *74*, 229.
(9) Hennig, J.; Limbach, H. H. *J. Magn. Reson.* **1982**, *49*, 322.
(10) Limbach, H. H.; Hennig, J.; Stulz, J. *J. Chem. Phys.* **1983**, *78*, 5432.
(11) Stilbs, P.; Moseley, M. E. *J. Chem. Soc., Faraday Trans. 2* **1980**, *76*, 729.
(12) Yeh, H. C.; Sato, M.; Morishima, I. *J. Magn. Reson.* **1977**, *26*, 365.
(13) Irving, C. S.; Lapidot, A. *J. Chem. Soc., Chem. Commun.* **1977**, 184.
(14) Limbach, H. H. *J. Magn. Reson.* **1979**, *36*, 1979.
(15) Limbach, H. H.; Seiffert, W. *J. Am. Chem. Soc.* **1980**, *102*, 538.
(16) Gerritzen, D.; Limbach, H. H. *Ber. Bunsenges. Phys. Chem.* **1981**, *85*, 527.
(17) Bachovchin, W. W.; Roberts, J. D. *J. Am. Chem. Soc.* **1978**, *100*, 8041.
(18) Hilbers, C. W. In "Biological Application of Magnetic Resonance", Academic Press: New York, 1979; Chapter 1.
(19) Rueterjans, H.; Kaun, E.; Hull, W.; Limbach, H. H. *Nucleic Acid Res.* **1982**, *10*, 7027.
(20) DiVerdi, J. A.; Opella, S. J. *J. Am. Chem. Soc.* **1982**, *104*, 1761.
(21) Boxer, S. G.; Closs, G. L.; Katz, J. J. *J. Am. Chem. Soc.* **1974**, *96*, 7058.
(22) Kuroda, Y.; Lee, H. Kuwae, A. *J. Phys. Chem.* **1980**, *84*, 3417.
(23) Martin, G. J.; Martin, G. L.; Gouesnard, J. P. "^{15}N Spectroscopy"; Springer: Berlin, 1981.
(24) Jackman, L. M.; Trewella, J. C. *J. Am. Chem. Soc.* **1976**, *98*, 5712; **1979**, *101*, 6428.
(25) Silvers, S. J.; Tulinsky, A. *J. Am. Chem. Soc.* **1967**, *89*, 3331.
(26) Tulinsky, A. *Ann. N.Y. Acad. Sci.* **1973**, *206*, 47.
(27) Hamor, M. J.; Hamor, T. A.; Hoard, J. L. *J. Am. Chem. Soc.* **1964**, *86*, 1938.
(28) Webb, L. E.; Fleischer, E. B. *J. Chem. Phys.* **1965**, *43*, 3100.
(29) Hoskins, B. F.; Mason, S. A.; White, J. C. B. *J. Chem. Soc., Chem. Commun.* **1969**, 554.
(30) Adler, A. D.; Longoi, F. R. *J. Org. Chem.* **1967**, *32*, 476.
(31) Van Geet, A. L. *Anal. Chem.* **1970**, *42*, 675.
(32) Farrar, T. C.; Becker, E. D. "Pulse and Fourier Transform NMR"; Academic Press: New York, 1971.

operates between 6 and 10 MHz was increased from 10 to 16 mm at the expense of the resolution. Figure 1 shows some typical ^{15}N NMR spectra of TPP as a function of the temperature. As described by Gust et al.,[5] two ^{15}N signals are obtained at low temperatures. The low-field signal corresponds to the nonprotonated nitrogen atoms (N_3, N_6 in eq 1) and the high field signal to the protonated nitrogen atoms (N_2, N_5 in eq 1) because this signal is split into a doublet when the spectra are recorded at low temperatures without ^1H decoupling. No attempt was made to determine the absolute chemical ^{15}N shifts of these signals. We find a chemical shift difference for these signals in toluene-d_8 of 130.5 ppm, which is greater than the value of 107 ppm reported by Gust et al.[5] for $CDCl_3$. We will comment on the interesting behavior of the ^1H-decoupled spectra as a function of the temperature in the next section. The NOE were determined as follows: each free induction decay signal was Fourier transformed several times with a different value of artificial line broadening LB. Assuming a Lorentzian line shape the peak height PH_i of the signal i is then given by

$$PH_i = I/(W_{0i} + LB) \tag{2}$$

By nonlinear least-squares fitting, the two parameters in eq 2, the intensity I and the width W_{0i} of the line i, were determined. If I_c and I_{ss} are the signal intensities for the proton coupled and the proton decoupled (steady-state) signal, the steady state NOE of the line i is given by[23]

$$\eta_i^{ss} = (I_{ss} - I_c)/I_c \tag{3}$$

The doublet structure of the undecoupled NH signal was taken into account. The values of I determined according to eq 2 are not influenced by small unresolved long-range $^1H^{15}N$ couplings. The accuracy of the NOE values determined by the procedure described in eq 2 is limited by the poor signal to noise ratio at low values of LB; however, the relative NOE of the two signals are much more accurate. ^{15}N-T_1 values were determined at low temperature using the inversion recovery method.[32] An example is shown in Figure 2. This method was not useful at high temperatures where the T_1 of the coalesced ^{15}N signal were quite long. Therefore, the progressive saturation method was applied at high temperatures.[32]

Evaluation of the Experimental Data

In order to calculate the T_1 and steady-state NOE as a function of the temperature several assumptions had to be made: (i) the longitudinal relaxation of the central protons, whose signal shows spin–spin splitting by scalar coupling to the ^{15}N atoms can be described by an effective relaxation time which is approximately the true T_1; (ii) each of the central protons is entirely relaxed by the other proton and by its immediate ^{15}N neighbor; (iii) the β-pyrrole protons relax each other; (iv) in the absence of proton exchange the ^{15}N nuclei are relaxed by the central protons and by the chemical shift anisotropy (CSA) relaxation mechanism. As was shown by Werbelow et al.,[33] the error induced by using assumption (i) is not greater than 15%; i.e., this assumption holds within our margin of error unless there is an extreme motional anisotropy and as long as no soft pulses are applied to individual lines. Assumption (ii) will be verified as shown below by comparison of the experimental and the calculated T_1 data.

The nuclear spin relaxation behavior of an ellipsoid undergoing anisotropic rotational Brownian motion has been described by Woessner.[34] We take TPP as a symmetric top molecule characterized by two rotational correlation times $\tau_\perp$ and $\tau_\parallel$, where $\parallel$ is the axis perpendicular to the molecular plane. We obtain from Woessner's equations the following expression for the spectral densities describing the reorientation of a vector which lies in the molecular plane as do the $^1H^{15}N$ and the HH vectors

$$J(\omega) = \frac{1}{4}\left[\frac{\tau_\perp}{1 + \omega\tau_\perp{}^2} + \frac{9\tau_\perp/(2\alpha + 1)}{1 + \omega^2(3\tau_\perp/(2\alpha + 1))^2}\right] \tag{4}$$

where

$$\alpha = \tau_\perp/\tau_\parallel \tag{5}$$

is the rotational asymmetry factor. The dipole–dipole relaxation times of spin $^1/_2$ nuclei are given by[35-37]

$$\frac{1}{T_{1I}^{DD}} = \rho_I^{DD} = D[J_0(\omega_I - \omega_S) + 3J_1(\omega_I) + 6J_2(\omega_I + \omega_S)] \tag{6}$$

for the heteronuclear case and by

$$\frac{1}{T_{1I}^{DD}} = \rho_I^{DD} = 3D[J_1(\omega_I) + 4J_2(2\omega_I)] \tag{7}$$

for the homonuclear case, where

$$D = \frac{1}{10}\frac{\gamma_I^2\gamma_S^2\hbar^2}{\langle r_{IS}^3\rangle^2} \tag{8}$$

The CSA relaxation times are given by[32]

$$\frac{1}{T_{1I}^{CSA}} = \rho_I^{CSA} = \frac{2}{15}\omega_I^2\Delta\sigma_I^2 J_1(\omega_I) \tag{9}$$

and the Nuclear Overhauser Enhancement factors by[35-37]

$$\eta_I = \frac{D[6J_2(\omega_I + \omega_S) - J_0(\omega_I - \omega_S)]}{\rho_I^{DD} + \rho_I^{res}}\frac{\gamma_S}{\gamma_I} \tag{10}$$

$\Delta\sigma_i$ is the chemical shift anisotropy of the nucleus, i, $\hbar = h/2\pi$, where h is Planck's constant. γ_i is the gyromagnetic ratio of nucleus i. ρ^{res} is the nondipolar contribution to the relaxation rate. ω is the Larmor frequency of the nucleus i, $\langle r_{ij}^3\rangle^{-1/3}$ is the mean cubic distance between atoms i and j representing an average over all vibrational states. The temperature dependence of $\tau_\perp$ is given by an Arrhenius law

$$\tau_\perp = \tau_{0\perp}\exp(E_a/RT) \tag{11}$$

where R is the gas constant and T is the temperature. In eq 11 it is assumed (assumption v) that α is independent of the temperature, i.e., $E_{a\perp} = E_{a\parallel} = E_a$.

Equations 6, 7, 9, and 10 are valid only in the absence of chemical exchange. The problem of T_1 and NOE measurements in the presence of chemical exchange has been studied by several authors.[9,39-45] In their discussion of selective T_1 measurements, Campbell et al.[43] took into account NOE effects between mutually dipolar coupled spins which exchange at the same time. The case presented here of two exchanging spins $^1/_2$ (the ^{15}N atoms) which are coupled to additional spins 1/2 (the central protons of TPP) has, to our knowledge, not yet been discussed although the solution to this problem is straightforward. The modified Bloch equations for two exchanging spins can be written in the absence of mutual dipolar coupling[38,39] (assumption vi)

$$\frac{dI}{dt} = -\rho_I(I - I_\infty) + k_{SI}S - k_{IS}I \tag{12}$$

$$\frac{dS}{dt} = -\rho_S(S - S_\infty) + k_{IS}I - k_{SI}S \tag{13}$$

I and S are the magnetization of the two spins at the time t, ρ_i is the inverse T_1, k_{IS} and k_{SI} are the rate constants, and I_∞ and S_∞ are the equilibrium magnetizations in the presence of decoupling of the spins to which I and S are dipolar coupled, here of

(33) Werbelow, L. G.; Grant, D. M. *J. Chem. Phys.* **1975**, *63*, 544.
(34) Woessner, D. E. *J. Chem. Phys.* **1962**, *37*, 647.
(35) Bloembergen, N.; Purcell, E. M.; Pound, R. V. *Phys. Rev.* **1948**, *73*, 679.
(36) Abragam, A. "The Principles of Nuclear Magnetism"; Clarendon Press: Oxford, 1961; Chapter 8.
(37) Noggle, J. H.; Schirmer, R. E. "The Nuclear Overhauser Effect"; Academic Press: New York, 1971.
(38) Solomon, I. *Phys. Rev.* **1955**, *99*, 559.
(39) McConnell, H. M. *J. Chem. Phys.* **1958**, *28*, 430.
(40) Levy, G. C.; Nelson, G. L. *J. Am. Chem. Soc.* **1974**, *94*, 4897.
(41) Strehlow, H.; Frahm, J. *Ber. Bunsenges. Phys. Chem.* **1975**, *79*, 57.
(42) Gerhard, R.; Dietrich, W. *J. Magn. Reson.* **1976**, *23*, 21.
(43) Campbell, I. D.; Dobson, C. M.; Ratcliffe, R. G.; Williams, R. J. P. *J. Magn. Reson.* **1978**, *29*, 397.
(44) Lambert, J. B.; Keepers, J. W. *J. Magn. Reson.* **1980**, *38*, 233.
(45) Borzo, M.; Maciel, G. E. *J. Magn. Reson.* **1981**, *43*, 175.

the ^1H nulcei. Since I_c and S_c are the equilibrium magnetizations in the absence of decoupling, one can write

$$\eta_I = \frac{I_\infty - I_c}{I_c} \tag{14}$$

η_I is the true NOE of I in the absence of exchange. The following relation holds

$$\frac{I_c}{S_c} = \frac{k_{SI}}{k_{IS}} = K \tag{15}$$

where K is the equilibrium constant.

The solution of eq 12 and 13 can be written in the form[41-43]

$$I = A_+ \exp(\Lambda_+ t) + A_- \exp(\Lambda_- t) + I_{ss} \tag{16}$$

$$S = B_+ \exp(\Lambda_+ t) + B_- \exp(\Lambda_- t) + S_{ss} \tag{17}$$

$$\Lambda_\pm = \frac{1}{2}(-\rho_I - \rho_S - k_{IS} - k_{SI}) + \frac{1}{2}\{[\rho_I - \rho_S + k_{IS} - k_{SI}]^2 + 4k_{IS}k_{SI}\}^{1/2} \tag{18}$$

$$A_\pm = \frac{1}{\Lambda_+ - \Lambda_-}[\pm(I_{ss} - I_0)(\rho_I + k_{IS} + \Lambda_\mp) \mp k_{SI}(S_{ss} - S_0)] \tag{19}$$

$$B_\pm = \frac{1}{\Lambda_+ - \Lambda_-}[\mp(S_{ss} - S_0)(\rho_I + k_{IS} + \Lambda_\pm) \mp k_{IS}(I_{ss} - I_0)] \tag{20}$$

For a nonselective inversion recovery experiment,[43] the magnetizations I_0 and S_0 and $t = 0$ are equal to $-I_{ss}$ and $-S_{ss}$. The steady-state magnetizations I_{ss} and S_{ss} are obtained by setting eq 12 and 13 to zero

$$I_{ss} = \frac{\rho_I(\rho_S + k_{SI})I_\infty + \rho_S k_{SI} S_\infty}{(\rho_I + k_{IS})(\rho_S + k_{SI}) - k_{IS}k_{SI}} \tag{21}$$

As shown in the literature,[40-44] the effective relaxation rates are given in the range where k_{IS}, $k_{SI} \gg \rho_I$, ρ_S by

$$\rho_I^{eff} = \rho_S^{eff} = \frac{1}{2}(\rho_I + \rho_S) \tag{22}$$

It follows that for $\rho_S \ll \rho_I$

$$\rho_I^{eff} = \rho_S^{eff} = \frac{1}{2}\rho_I \tag{23}$$

When the exchange rate constants become very small it follows[40-44] from eq 16–20 that

$$\rho_I^{eff} = -\Lambda_+ = \rho_I + k_{IS} \approx \rho_I \tag{24}$$

$$\rho_S^{eff} = -\Lambda_- = \rho_S + k_{SI} \approx \rho_S \tag{25}$$

By combination of eq 3, 14, 15, and 21 one obtains for the steady-state NOE in the presence of exchange

$$\eta_I^{ss} = \frac{\rho_I(\rho_S + k_{SI})\eta_I + \rho_S k_{IS}\eta_S}{(\rho_I + k_{IS})(\rho_S + k_{SI}) - k_{IS}k_{SI}} \tag{26}$$

A similar equation is obtained for η_S^{ss} by interchanging I and S. We discuss eq 26 in terms of proton transfer equilibria involving ^{15}N atoms. Consider a nitrogen atom which absorbs in the NH region and which is involved in the reaction

$$\underset{(I)}{NH} + X \rightleftharpoons \underset{(S)}{N} + HX \tag{27}$$

To a good approximation, $\rho_I \gg \rho_S$ and $|\eta_I| \gg |\eta_S|$; therefore, it follows from eq 26 for the fast exchange case ($k_{SI} \gg \rho_S$) that

$$\eta_I^{ss} = \eta_I/(1 + K\rho_S/\rho_I) \approx \eta_I \tag{28}$$

and for the slow exchange case ($k_{SI} \ll \rho_S$) that

$$\eta_I^{ss} = \eta_I/(1 + k_{IS}/\rho_I) \approx \eta_I \tag{29}$$

Thus, the steady-state NOE of a proton bonded nitrogen signal is almost equal to its true NOE; i.e., it is not much affected by the exchange process. The behavior of nonprotonated nitrogen atoms which are involved in the reaction

$$\underset{(I)}{N} + HX \rightleftharpoons \underset{(S)}{NH} + X \tag{30}$$

is, however, different. Here we have to a good approximation that $\rho_I \ll \rho_S$ and $|\eta_I| \ll |\eta_S|$. For the case of a degenerate reaction ($K = 1$) we obtain

$$\eta_I^{ss} = k\eta_S/(\rho_I + k) + \eta_I \tag{31}$$

from which it follows that $\eta_I^{ss} \approx \eta_S$ for $k \gg \rho_I$ and $\eta_I^{ss} = \eta_I$ for $k \ll \rho_I$. This means that if the exchange is fast enough (although not too fast for the coalescence of the two line I and S to occur) the line of the nonprotonated nitrogen atom (I) experiences the NOE of the protonated atom (S). However, it experiences its own NOE which is close to zero when the exchange becomes very slow. For the unsymmetrical case ($K \ll 1$) we obtain for $k_{SI} \gg \rho_S$

$$\eta_I^{ss} = \frac{\rho_S}{\rho_I} K\eta_S + \eta_I \tag{32}$$

and for $k_{SI} \ll \rho_S$

$$\eta_I^{ss} = \frac{k_{IS}}{\rho_I}\eta_S + \eta_I \approx \eta_I \tag{33}$$

From eq 32 it follows that the steady-state NOE of a nitrogen atom (I) in eq 30 should be proportional to the equilibrium constant K of the tautomerism.

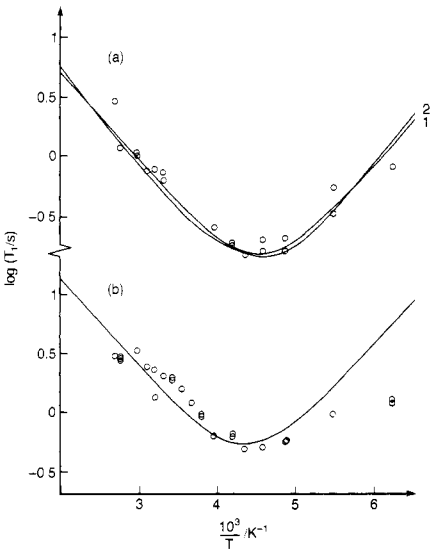

Figure 3. Log T_1 values of the central protons (a) and of the β-pyrrole protons (b) in toluene-d_8 at 90.02 MH as a function of the inverse temperature. The curves were described in the text. Curve 1 (a): $\alpha = 1$, isotropic motion; curve 2 (a): anisotropic motion with $\alpha = 5$.

Results

The results of our T_1 and NOE measurements are gathered in Table I and in Figures 3 and 4. The parameters describing the calculated curves in Figures 3 and 4 are given in Table II. A minimum in the ^1H-T_1 values of the central protons and of the β-pyrrole protons occurs at about 220 K. In the same temperature region the negative NOE of the ^{15}N signal disappears. This is consistent with a dominant ^1H–^{15}N dipole–dipole relaxation mechanism for the ^{15}N nuclei. Each central proton is relaxed by the other central proton and by the adjacent ^{15}N spin. The relaxation data of these protons were, therefore, calculated in terms of a sum of eq 6 and 7, i.e. by varying the two static parameters r_{12}, r_{14}, and the three dynamic parameters α, E_a, and $\tau_{0\perp}$. We note that the form of the curve is determined, in practice, by the dynamic variables. The distances r_{12} and r_{14} determine the value of T_1 in the minimum. Values of $\alpha \neq 1$ lead to asymmetric log

Table I. Experimental Longitudinal Relaxation Times (s) ^{1}H-T_1 at 90.02 MHz, ^{15}N-T_1, and NOE values at 9.12 MHz of $^{15}N_4$ TPP in Toluene-d_8

T/K	a	b	T/K	a	b
373	3.07	2.93	264	0.98	
363	2.80	1.19	264	0.94	
363	2.86		253	0.65	
363	2.91	1.20	253	0.645	0.256
363	3.02		239	0.67	0.18
337	3.4	1.09	239	0.64	0.19
323	2.48	0.77	230	0.50	0.148
313	1.36		230	0.51	
313	2.34	0.79	219	0.53	0.2
303	2.10	0.74	219	0.52	0.16
303	2.07	0.64	206	0.59	0.16
293	2.04		206	0.58	0.21
293	1.89		205	0.60	
283	1.59		183	1.0	0.55
283	1.59		183		0.34
273	1.23		171	1.34	
273	1.23		171	1.23	0.83

T/K	c	d	e	f
382		4.9		
374		4.0		
358		4.4	−3.5	
200			−2.3	−2.4
197			−1.1	−0.6
190			−0.3	−1.0
180	0.67	0.05	−0.1	−0.7

[a] ^{1}H-T_1 values of the β-pyrrole signals. [b] ^{1}H-T_1 values of the central protons. [c] ^{15}N-T_1 values of the protonated nitrogen N_2/N_5 atoms. [d] ^{15}N-T_1 of the nonprotonated N_3/N_6 atoms. [e,f] Nuclear enhancement factors η of the N_3/N_6 and of the N_2/N_5 signals.

T_1 vs. $1/T$ curves.[34] Curve fitting as shown in Figure 3a enabled us for a given value of α and r_{12} to extract the parameters r_{14}, E_a, and $\tau_{\perp 0}$ from the experimental data. A comparison of curve 1 and 2 in Figure 3a shows that even a value of $\alpha = 5$ leads only to a small asymmetry around the T_1 minimum. This is also true for values of $\alpha = 0.2$. Our data are, thus, consistent with the range of dynamic parameters given by the first three entries in Table II; r_{12} and r_{14} were almost independent on the choice of α. Since we were mainly interested in the position of the central H atoms we set $\alpha = 1$ in the subsequent analysis. As mentioned above, the ^{1}H-T_1 data of the central protons can be explained by different pairs of r_{12} and r_{14} values. The range of possible values is given by entries no. 4 to 9 in Table II. The analysis of the ^{15}N-T_1 data displayed in Figure 4 gave, however, additional information concerning the value of r_{12} and, thus, of r_{14} as shown in the following. The ^{15}N-T_1 values in the absence of chemical exchange were calculated in terms of a superposition of eq 6 and 9, i.e., in terms of a superposed ^{1}H^{15}N dipole–dipole and CSA relaxation mechanism. Equation 6 was multiplied by a factor of 2 in the calculation of the T_1 values for the nonprotonated ^{15}N atoms because they are partly relaxed by two central protons. Since we

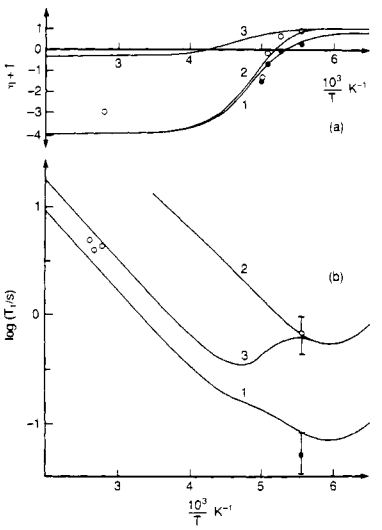

Figure 4. Experimental Nuclear Overhauser Effects (NOE) η + 1 (a) and apparent ^{15}N-T_1 values (b) of $^{15}N_4$-TPP in toluene-d_8 at 9.12 MHz as a function of the inverse temperature: (○) low-field signal; (●) upfield signal. The curves were calculated as described in the text. Curve 1 (a): NOE of the upfield; curve 2 (a): NOE of the low-field signal; curve 3 (a): intrinsic NOE of the low-field signal; curve 1 (b): upfield signal, curve 2 (b): low-field signal; curve 3 (b): effective T_1.

already knew the dynamic parameters E_a and $\tau_{0\perp}$ from the analysis of the ^{1}H-T_1 data, only r_{12}, r_{13}, $\Delta\sigma_2$, and $\Delta\sigma_3$ had to be varied for the calculation of the N_2-T_1 (curve 2 in Figure 4b) and the N_3-T_1 data (curve 2 in Figure 4b). The CSA relaxation mechanism was found to be negligible for the protonated N_2 atoms when r_{12} was on the order of 1 Å and when $\Delta\sigma_2$ was varied between 0 and 800 ppm. By contrast, the CSA relaxation mechanism dominated over the dipole–dipole relaxation mechanism for the nonprotonated N_3 atoms in the absence of chemical exchange for typical values of the order of $r_{13} = 2$ Å and $\Delta\sigma_3 > 400$ ppm. The actual value of $r_{13} = 2.33$ Å was estimated from the crystallographic data and $\Delta\sigma_3$ was adjusted in a way that curve 2 in Figure 4b reproduced the experimental low temperature value. Curve 3 in Figure 4b represents Λ^{-1} in eq 18 and describes the effective relaxation times of the coalesced signal at high temperatures and of the nonprotonated N atoms at low temperatures. For the calculation of curve 3 the experimental proton exchange rates[8]

$$k = 10^{10.9} \exp(-4787/T) \qquad (34)$$

where used as well as the parameters of curves 1 and 2 in Figure 4b. At high temperatures eq 23 holds, and curves 1 and 3 differ only by a factor of 2. The experimental data should be described in this temperature region by curve 3. Moreover, because of the dominance of the ^{1}H^{15}N dipole–dipole relaxation mechanism the ^{15}N-T_1 depend only on one static parameter, the distance r_{12}. Knowledge of the dynamic parameters enables us, therefore, to extract r_{12} by fitting—as represented by curve 3 in Figure 4b—to

Table II. Parameters Used for the Calculation of the T_1 and NOE Data Shown in Figures 3 and 4 (For the Numbering of the Atoms See Eq 1. For Explanation of Symbols See Text.)

		figure	curve	eq	r_{12}/Å	r_a/Å	r_{13}/Å	r_{14}/Å	$\Delta\sigma_3$/ppm	α	$\tau_{0\perp}$/ps	E_a/kJ mol^{-1}
1	H_1 T_1	3a	1	6 + 7	1.02			2.4		1	0.677	14.13
2	H_1 T_1	3a	2	6 + 7	1.02			2.4		0.2	0.336	14.13
3	H_1 T_1			6 + 7	1.00			2.3		5	0.749	15.79
4	H_1 T_1			6 + 7	0.96			3.7		1	0.677	14.13
5	H_1 T_1			6 + 7	0.98			2.6		1	0.677	14.13
6	H_1 T_1			6 + 7	1.00			2.38		1	0.677	14.13
7	H_1 T_1			6 + 7	1.04			2.30		1	0.677	14.13
8	H_1 T_1			6 + 7	1.06			2.25		1	0.677	14.13
9	H_1 T_1			6 + 7	1.20			2.1		1	0.677	14.13
10	H_a T_1	3b		6		2.49				1	0.677	14.13
11	N_2 T_1	4b	1	6	1.02					1	0.677	14.13
12	N_2 NOE	4a	1	10	1.02					1	0.677	14.13
13	N_3 T_1	4b	2	6 + 9			2.33		660	1	0.677	14.13
14	N_3 NOE	4a	2	10			2.33		660	1	0.677	14.13

our high-temperature relaxation times. By setting r_{12} = 0.96 Å, we would obtain the best agreement between the calculated and the experimental values. However, as shown in Table II entry no. 4, the value of r_{14} would then be more than 1 Å too high as estimated from the crystallographic data. In order to decrease r_{14} to values which are compatible with the TPP structure, we have to increase r_{12} only very slightly. When we do this the calculated high temperature ^{15}N-T_1 value increases. The maximum value of r_{12} which is able to reproduce the experimental data within the margin of error is about 1.03 Å. Actually, curve 3 in Figure 4b was calculated using r_{12} = 1.02 Å (entry no. 11 in Table II). In any case, a further increase of r_{12} reduces r_{14} only very slightly as shown by entries no. 6–11 in Table II. Thus, we adopt the pair of values r_{12} = 1.02 Å and r_{14} = 2.4 Å as the one which is in best agreement with the relaxation times and the chemical structure of TPP. Using the values given by entry no. 11 in Table II, curve 1 in Figure 4b also reproduces quite well the low temperatures N_2-T_1 value within the margin of error. Finally, we now have all parameters needed to calculate the NOE as a function of temperature using eq 26 and 34. The results are shown in Figure 4a. Curve 1 represents the steady-state NOE of the protonated nitrogen atoms which is almost identical with its true NOE as expressed by eq 28 and 29. The steady-state and the true NOE of the nonprotonated nitrogen atom are represented by curves 2 and 3 in Figure 4a. They differ much more and behave as predicted by eq 31. In view of the fact that we did not vary any parameter in the calculation of the steady state NOE curves—which are, thuse, entirely predicted by the preceding analysis—the agreement with the experimental data is excellent.

In the last stage we calculated the T_1 data of the β-pyrrole protons H_a and H_b. Although at low temperature two signals are observed for these protons the T_1 values were found to be equal. In Figure 3a the experimental data and those calculated using the known dynamic parameters as well as a value of r_{ab} = 2.49 Å (entry no. 10 in Table II) are compared. Besides the two low temperature values the fit is very satisfactory.

Discussion

In the preceding section we were able to explain the relaxation data of TPP in toluene-d_8 in terms of the molecular structure using the following relaxation picture. About two thirds of the relaxation of each inner proton is caused by dipole–dipole relaxation with the ^{15}N atom to which it is attached and one third by dipole–dipole relaxation with the other central proton. Each protonated $^{15}N_2$ spin is fully relaxed by dipole–dipole relaxation to the attached proton. The intrinsic T_1 of the nonprotonated $^{15}N_3$ spins are much smaller by comparison. Below the coalescence point of the two ^{15}N signals—which lies at about room temperature—and above the T_1 coalescence region—which begins at about −50 °C—the N_3 spins are relaxed by magnetization transfer to the N_2 spins via the hydrogen migration, which provides an indirect relaxation pathway for dipole–dipole relaxation with the inner protons. Below −90 °C the proton transfer rates and, therefore, the magnetization transfer rates are smaller than the intrinsic N_3-T_1 relaxation times. In this region the N_3 atoms are dominantly relaxed by the CSA relaxation mechanism and to a minor extent by a direct dipole–dipole relaxation to the two inner hydrogens. This behavior has the following consequences for the NOE as a function of temperature. Above room temperature we observe a negative NOE of the coalesced signal which is within the margin of error close to the maximum NOE of −4.93. Below the coalescence point of the two nitrogen signals, each line experiences the same negative NOE as long as the magnetization transfer rates are fast enough, although the intrinsic NOE of the nonprotonated N nuclei is quite small as expressed by curve 3 in Figure 4a. Due to the slow proton exchange below −60 °C, the negative NOE of this signal decreases, the signal vanishes, and finally becomes positive as the temperature is further lowered. The NOE curve is very sensitive in this region to the proton exchange rate constant k, i.e., in the region where k^{-1} is on the order of the intrinsic N_3-T_1 value. Thus, it is possible to obtain very small proton exchange rate constants by ^{15}N NMR measurements where ^1H or ^{13}C NMR spectroscopy fails. The observation that magnetization transfer between the two nitrogen atoms ceases in this temperature region indicates that cross relaxation between these two atoms is negligible; i.e., assumption (vi) holds. At even lower temperatures, the negative NOE of the NH signal also breaks down because the T_1 minimum is approached. In a more favorable case than TPP, the NOE breakdown of the two signals might take place in totally different temperature regions.

The observation of a ^1H-T_1 minimum around 220 K is consistent with our previous[6] observation of different longitudinal and transverse relaxation rates in this temperature region, which is a consequence of the minimum.[34,35] This difference does, therefore, not arise from the proton transfer.[9,11]

We want now to compare the distances derived in the preceding section with those obtained by analysis of the crystal structure in the solid state.[25-29] By X-ray crystallographic analysis, Silvers and Tulinsky[25,26] have found an NH distance of r_{12} = 0.86 Å and an HH distance of r_{14} = 2.41 Å for porphine. The hydrogen atoms were found slightly above the molecular plane. The same authors[25] reported values of r_{12} = 0.93 Å and r_{14} = 2.36 Å for triclinic TPP which also shows a small distortion of the molecular plane due to intermolecular interactions. There was also a small deviation of the position of the hydrogen atoms from the N···N axis. In order to overcome the problem of an exact proton localization by X-ray analysis, Hoskins et al.[29] have carried out a neutron diffraction study of phthalocyanine which is structurally very close to the porphines. They found an NH distance of r_{12} = 0.94 Å and reported an uncertainty of 0.05 Å for this value. As a consequence, we state that our values of r_{12} = 1.02 Å and r_{14} = 2.4 Å are in very good agreement with those obtained from the crystal studies, although there seems to be a small systematic difference between the r_{12} values. For a discussion of this small difference we have, however, to keep two facts in mind. The first is that X-ray analysis underestimates XH distances.[25-29] The second is that the distances which appear in the expressions for the dipole–dipole relaxation such as eq 8 are mean cubic vibrationally averaged distances $r = \langle r^3 \rangle^{1/3}$, which may be some percent larger than the average distances when hydrogen atoms are involved.[46-49] Diehl et al.[46] found a 5% difference for the corresponding CH distances in benzene. We estimate for TPP a similar correction factor which would result in a vibrationally corrected NH value of about 0.97 Å which is now in much better agreement with the solid state studies. We estimate that our HH distance r_{14} also needs some vibrational correction which would reduce its value in a way that a linear NH···HN arrangement—as found for phthalocyanine[29]—seems also to be possible for TPP in solution. An exact calculation of the correction factors requires, however, a normal coordinate analysis of TPP in solution and is beyond the scope of this study. The fact that we were able to get reasonable r_{12} and r_{14} values from our relaxation data encouraged us to take the crystallographic distance r_{13} = 2.33 Å in order to calculate the dipole–dipole contribution to the intrinsic N_3-T_1. As mentioned in the preceding section, this determines the small intrinsic NOE of N_3. This intrinsic NOE of N3 could not be determined directly because of the magnetization transfer. The reliability of the value for $\Delta\sigma_3$ = 660 ppm should, however, not be overestimated because this value depends on the accuracy of the experimental N_3-T_1 and the assumed distance for r_{13}. From preliminary solid state ^{15}N experiments[50] on TPP we estimate $\Delta\sigma_3$ to lie between 300 and 700 ppm which is consistent with the proposed value. An additional argument in favor of our interpretation of the NOE comes from a discussion of the proton decoupled 9.12-MHz ^{15}N NMR spectra of pheophytin-$^{15}N_4$ measured by Boxer et al.[21] Four different ^{15}N signals were observed for this unsymmetrically substituted free base porphine which indicates that the tautomerism according to eq 1 is no more

(46) Diehl, P.; Niederberger, W. *J. Magn. Reson.* **1973**, *9*, 495.
(47) Cyvin, S. J. "Molecular Vibrations and Mean Squares Amplitudes"; Elsevier: Amsterdam, 1968.
(48) Bastiansen, O.; Traetteberg, M. *Acta Cryst.* **1960**, *13*, 1108.
(49) Morino, Y. *Acta Cryst.* **1960**, *13*, 1107.
(50) Limbach, H. H.; Yannoni, C. S.; Kendrick, R., unpublished results.

degenerate; in other words, only one tautomer is present. The two protonated ^{15}N atoms experienced a large negative NOE whereas the nonprotonated atoms experienced only a small negative NOE, which was of the order of the value which we have calculated for N_2 in TPP at high temperatures (Figure 4a, curve 3). We may take this coincidence as a further argument for the plausibility of this value. We can, however, not exclude that this small negative NOE arises from the presence of a small amount of the energetically more unfavorable tautomer, as predicted by eq 32. One may, however, distinguish between the two possibilities. If the NOE of the nonprotonated nitrogen atoms in pheophytin would arise from the presence of a second tautomer, it should increase with increasing temperature because one expects the equilibrium constant to increase. If the NOE is caused by direct dipole–dipole interaction of the nonprotonated nitrogen atoms with the central proton, it should be almost independent of the temperature as indicated by curve 3 in Figure 4a. In order to decide this question it would be necessary to carry out temperature-dependent ^{15}N studies of pheophytin or similar unsymmetrical porphines.

From the preceding discussion, it is clear that an inclusion of additional relaxation mechanisms, e.g., dipole–dipole relaxation caused by paramagnetic impurities, would lead to greater NH and HH distances which are no longer consistent with the structural data. In addition, we would not find T_1 values for the two kinds of ^{15}N atoms which differ by a factor of the order of 10 at low temperatures.

The last static parameter we have to discuss is the value of r_{aa} = 2.49 Å which describes the dipolar relaxation between the pairs of β-pyrrole protons. From the crystallographic data of TPP,[25] we expect a value of about 2.6–2.7 Å which is of the same order, although a bit higher. Therefore, we cannot exclude that assumption (iii) does not exactly hold; i.e., the β-pyrrole protons may be partly relaxed by another proton, for example, the *o*-phenyl proton.

So far we have discussed the static parameters derived from the data, and come now to a discussion of the dynamic parameters E_a, $\tau_{0\perp}$, and α which, as defined by eq 5 and 11, characterize the motion of the molecule. Our data could be explained by an isotropic motion with $\alpha = 1$ as well as by an anisotropic motion with values as low as 0.2 or as high as 5. Considering the more pancake-like structure of the TPP molecule, one would expect values of greater than 1 because rotation about an axis which lies in the molecular plane requires more solvent displacement than rotation about the axis perpendicular to the molecular plane. As shown in the preceding section, the static parameters derived from our data did not significantly depend on the value of α in the range $0.2 < \alpha < 5$, because we were able to observe the T_1 minimum. If we had not observed this minimum, it would not have been possible to obtain the static parameters without assumptions concerning the dynamic parameters. The analysis was further facilitated by the fact that the NH and the HH vectors lie in the molecular plane. We want now ask whether the TPP rotation in toluene-d_8 may be described by the Stokes–Einstein–Debye model,[51] in which the rotational correlation times are given by

$$\tau = \xi \frac{V\eta^*}{kT} \tag{35}$$

where η^* is the viscosity of the solvent,[52] k is the Boltzmann constant, and ξ is a correction factor which is unity within the SED approach. Equation 35 indicates that the energy of activation of the molecular reorientation should be given by the value calculated from the curve ln T vs. $1/T$. From the known viscosity of toluene[52] we calculate a value of 13.2 kJ mol^{-1}. This value is in very good agreement with the values which we calculated from the relaxation data and which are given in Table II. Using eq 11 and 35 we calculated the molecular volume of TPP using the correlation times given in Table II. For T = 223 K which is near the T_1 minimum we obtain with η^* = 2.17 cP and $\tau_{0\perp}$ = 1360 ps a value of V = 1760 Å^3. At different temperatures, slightly different values are obtained which are, however, all greater than the volume of the basis cell unit of triclinic TPP[25] which is of the order of 800 Å^3. If one makes a correction according to Gierer and Wirtz,[53] the calculated volume increases about a factor of 2. When one uses the model of Hu and Zwanzig,[54] the volume increases again by a factor of about 2. However, because of our uncertainty in α we do not want to interpret these results further.

Conclusion

We have shown that it is possible to determine NH distances of proton transfer systems by the measurement of dipole–dipole relaxation rates by using a combination of ^1H and ^{15}N NMR spectroscopy without assumptions on the anisotropy of the molecular motion if the T_1 minimum can be observed. This minimum can be easily detected by the observation of an NOE breakdown of the ^{15}N signals. The detection of an NOE transfer between protonated and nonprotonated ^{15}N nuclei may be used to give information on the kinetics and thermodynamics of proton transfer between these atoms.

Acknowledgment. We are indebted to Dr. A. Kratochwill, University of Karlsruhe, and Dr. C. S. Yannoni, IBM Research Laboratory, San Jose, for helpful discussion, remarks, and reading of the draft. We also thank the Deutsche Forschungsgemeinschaft, Bonn-Bad Godesberg, and the Fonds der Chemischen Industrie, Frankfurt, for financial support.

Registry No. *meso*-Tetraphenylporphine, 917-23-7.

(51) For a recent review, see Boere, R. T.; Kidd, R. G. *Ann. Rep. Magn. Reson.* **1981**, *12*, 361.
(52) Barlow, A. D.; Laub, J.; Mathison, A. J. *Proc. R. Soc. London, Ser A* **1966** *292*, 322.
(53) Gierer, A.; Wirtz, K. *Z. Naturforsch.* **1953**, *A8*, 532.
(54) Hu, C. M.; Zwanzig, R. *J. Chem. Phys.* **1974**, *60*, 4354.